

## Data-Driven Shared Steering Control of Semi-Autonomous Vehicles

Huang, M.; Gao, W.; Wang, Y.; Jiang, Z.-P.

TR2019-020 May 23, 2019

### Abstract

This paper presents a cooperative framework of the driver and his/her semi-autonomous vehicle in order to achieve desired steering performance. In particular, a co-pilot controller and the driver operate together and control the vehicle simultaneously. Exploiting the classical small-gain theory, our proposed cooperative steering controller is developed independent of the unmeasurable internal states of human driver, and only relies on his/her steering torque. Furthermore, by adopting data-driven adaptive dynamic programming and an iterative learning scheme, the cooperative controller is learned from measurable data of the driver and the vehicle. Meanwhile, the accurate knowledge of the driver and the vehicle dynamics is unnecessary, which settles the problem of their potential parametric variations in practice. The effectiveness of the proposed method is validated by rigorous analysis and demonstrated by numerical simulations.

*IEEE Transactions on Human-Machine Systems*

This work may not be copied or reproduced in whole or in part for any commercial purpose. Permission to copy in whole or in part without payment of fee is granted for nonprofit educational and research purposes provided that all such whole or partial copies include the following: a notice that such copying is by permission of Mitsubishi Electric Research Laboratories, Inc.; an acknowledgment of the authors and individual contributions to the work; and all applicable portions of the copyright notice. Copying, reproduction, or republishing for any other purpose shall require a license with payment of fee to Mitsubishi Electric Research Laboratories, Inc. All rights reserved.



# Data-Driven Shared Steering Control of Semi-Autonomous Vehicles

Mengzhe Huang, Weinan Gao, *Member, IEEE*, Yebin Wang, *Senior Member, IEEE*, and Zhong-Ping Jiang, *Fellow, IEEE*

**Abstract**—This paper presents a cooperative framework of the driver and his/her semi-autonomous vehicle in order to achieve desired steering performance. In particular, a co-pilot controller and the driver operate together and control the vehicle simultaneously. Exploiting the classical small-gain theory, our proposed cooperative steering controller is developed independent of the unmeasurable internal states of human driver, and only relies on his/her steering torque. Furthermore, by adopting data-driven adaptive dynamic programming and an iterative learning scheme, the cooperative controller is learned from measurable data of the driver and the vehicle. Meanwhile, the accurate knowledge of the driver and the vehicle dynamics is unnecessary, which settles the problem of their potential parametric variations in practice. The effectiveness of the proposed method is validated by rigorous analysis and demonstrated by numerical simulations.

**Index Terms**—Shared driving, steering control, human in the loop, adaptive dynamic programming (ADP), small-gain.

## NOMENCLATURE

$\delta(\dot{\delta})$	Steering angle (rate)
$\zeta(\dot{\zeta})$	Driver's internal (error) state
$\eta_t$	Tire length contact
$\theta_{near}$	Near visual angle
$\theta_{far}$	Far visual angle
$\rho_i$	Curvature of road segment $i$
$\psi_L$	Heading angle error
$\psi_r$	Reference heading angle
$\psi_v$	Vehicle heading angle
$B_s$	Steering system damping
$C_f(C_r)$	Front (rear) cornering stiffness
$D_{far}$	Distance to the tangent point of road inner boundary
$I_s$	Steering system moment of inertia
$I_z$	Vehicle yaw moment of inertia
$K_a(K_c)$	Proportional gain to far (near) visual angle
$l_f(l_r)$	Distance from the center of gravity to front (rear) axle
$l_s$	Look-ahead distance
$m$	Mass of the vehicle

$r_a$	Yaw rate
$R_s$	Steering gear ratio
$T_d$	Driver's torque
$T_L(T_I)$	Lead (lag) time constant
$T_N$	Neuromuscular lag time constant
$T_i$	Driver's steady-state torque on road segment $i$
$u(\bar{u})$	Vehicle control input (error)
$v_x(v_y)$	Vehicle longitudinal (lateral) velocity
$x(\bar{x})$	Vehicle (error) state
$y_c$	Lane-keeping error at the center of gravity
$y_L$	Lateral offset from road centerline at look-ahead distance

## MATRICES AND VECTORS

$\mathcal{A}, \mathcal{B}$	Augmented state-space representation of the interconnected driver-vehicle system
$A, B, C, D$	State-space representation of the vehicle system
$A_d, B_d, C_d, D_d$	State-space representation of the driver system
$\mathcal{K}(\mathcal{K}^*)$	(Optimal) feedback control gain for $\mathcal{A}, \mathcal{B}$
$K(K^*)$	(Optimal) feedback control gain for $A, B$
$K_j$	Feedback control gain for $A, B$ at iteration $j$
$P^*$	Solution to the Riccati equation
$P_j$	Iterative solution to the Riccati equation at iteration $j$
$Q, r$	Weighting matrix and value
$\hat{U}_i$	Iterative solution to the regulator equation at iteration $i$
$X^*, U^*, Z^*$	Solutions to the regulator equations
$\hat{\mathcal{X}}$	Learned feedforward term approximating $X^*$

## I. INTRODUCTION

VEHICLE steering control has a variety of applications in the automotive industry and intelligent transportation systems. For an individual vehicle, a steering control system admits the great potential to improve its safety, such as collision avoidance system [1] and lane keeping system [2]. For connected vehicles equipped with communication devices, the steering control system is one of the demanding components to achieve the goal of platoon splitting and merging [3]. During the last few decades, vehicle steering control has been studied extensively for fully autonomous vehicles, while the human driver is replaced by the automation system

This work has been supported in part by the National Science Foundation under Grant ECCS-1501044, and in part by a gift from the Mitsubishi Electric Research Laboratories.

M. Huang and Z. P. Jiang are with the Control and Networks Lab, Department of Electrical and Computer Engineering, Tandon School of Engineering, New York University, Brooklyn, NY 11201 USA (e-mail: m.huang@nyu.edu; zjiang@nyu.edu).

W. Gao is with the Department of Electrical and Computer Engineering, Allen E. Paulson College of Engineering and Computing, Georgia Southern University, Statesboro, GA 30460 USA (e-mail: wgao@georgiasouthern.edu).

Y. Wang is with Mitsubishi Electric Research Laboratories, Cambridge, MA 02139 USA (e-mail: yebinwang@ieee.org).

and kept “out-of-the-loop”. The authors in [4], [5] point out that the driver’s awareness of the driving situation could be insufficient if he/she is not engaged in controlling the vehicle, which may lead to fatal accidents when the automation system is defective. In addition, a sudden transition from fully autonomous driving to manual driving is hard for the driver. This phenomenon has been observed in the experimental result shown in [6], where drivers’ steering performance was compromised during their adaptation to such a transition. Thus, in order to avoid such detrimental transitions or switches, the cooperative or shared control framework between driver and steering control system is encouraged, where the human driver is constantly involved in the task of driving.

To study the interaction between driver and steering assistance system, there is a significant number of important independent works in this field, such as shared control for advanced driver-assistance systems (ADAS) [7]–[14] and game theory for ADAS [15], [16]. Due to space limitation, we only cite and discuss some references that are closely related works to our paper. In [17], a two-point visual control model is proposed to illustrate the perception mechanism of a human driver during his/her driving. Essentially, it states that a driver usually fixates his/her focuses on two regions in front of the vehicle, and processes the received visual information. Then, he/she makes steering decisions so that the vehicle follows the lane centerline. Game-theoretic modeling approach has been utilized to formulate and settle the potential conflict of the driver’s interaction with the steering assistance system [16]. A predictive driver steering model is suggested in [18], where driver’s daily driving data are exploited to predict his/her behaviors in dangerous situations, e.g., collision avoidance. Taking advantage of these human driver modeling methods, researchers have proposed several cooperative steering control strategies for semi-autonomous vehicles in recent years. As shown in the literature, the general scheme of cooperative steering control is sketched in Fig. 1, where the steering assistance system collaborates with the driver by taking his/her steering command into consideration. In [7], a shared steering control is proposed to achieve lane keeping, taking the parametric uncertainty of the driver model into account. Model predictive control (MPC) strategies are adopted to combine the human driver and the vehicle into an overall system in order to complete steering maneuvers [8]–[10]. A novel steering ratio control technique is developed by [11] to assist driver in path following and to reduce driver’s workload. Recently, the authors in [12], [13] implement continuous control authority allocation between the driver and the vehicle, aiming to solve the conflict between human and machine.

Nonetheless, there are some practical issues arising from the implementation of shared steering control algorithms. Traditional model-based steering control strategies, which relies on the pre-identified models of drivers and vehicles, do not address both the adaptivity and optimality aspects, because driver’s behavior varies from person to person and from vehicle to vehicle. Additionally, those behaviors may change in the long term. From a control theoretical perspective, the heavy reliance on the accurate model dynamics potentially weakens the applicability of the shared steering controller. On the other

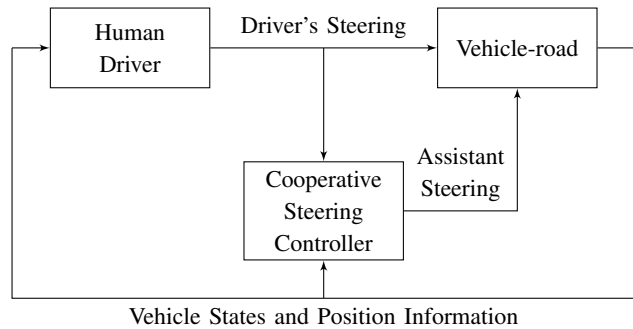


Fig. 1. Block diagram of cooperative steering control

hand, the absence of a precisely known model characterizing human behavior implies that the complex internal states of the driver cannot be acquired in the control implementation. This is also problematic for the most of the methods in the existing literature, e.g., [7], [9]. These limitations motivate our data-driven model-free approach for learning cooperative steering control laws online, which essentially does not rely upon the full knowledge of the driver and the vehicle.

This paper presents a data-driven learning strategy to design a cooperative steering controller using adaptive dynamic programming (ADP). ADP is a model-free method inspired by biological learning and control [19] and reinforcement learning [20]. It intends to iteratively learn the optimal controller in real time from measurable data without the accurate knowledge of system dynamics [21]–[26]. It should be mentioned that an integration of ADP and output regulation theory in [24], [26] has led to novel solutions to the design of adaptive and optimal tracking controllers with guaranteed disturbance rejection for linear and nonlinear uncertain systems. Applications of ADP have appeared in the data-driven adaptive optimal control of connected and autonomous vehicles [27], [28].

Because of the learning nature of ADP method, it might be confused with iterative learning control (ILC) [29], [30]. We here briefly state a few differences between them.

- 1) ILC updates the control signal (sequence) at the end of each trial in an off-line fashion [29], [30], while ADP, similar to adaptive control scheme, modifies the controller’s parameters in an online manner.
- 2) ILC intends to track a desired reference trajectory, and meanwhile the ADP method in this paper aims to solve a linear quadratic (LQ) optimal control problem. For example, in [31], the finite-horizon cost function to be minimized is defined using the tracking error and the difference of input sequences between two iterations. In our study, the performance index is infinite-horizon LQ, which tries to ensure performance and energy efficiency.
- 3) The optimization-based ILC relies on the model knowledge to update the control input at each iteration, see, e.g., [32]. On the contrary, ADP is a model-free method, which can learn the adaptive optimal controller from online data, without the model knowledge.

In this paper, we first formulate the steering control problem of a semi-autonomous vehicle with a human in the loop as a controller design problem for interconnected systems

comprised of the driver and his/her vehicle. Then, we develop a data-driven cooperative control policy for the interconnected human-vehicle system by means of robust adaptive dynamic programming (RADP) [25]. The objective of the steering control is to achieve lane keeping with minimum lateral deviation. Combining RADP and an iterative learning framework for the driver, an adaptive optimal steering controller is proposed to assist the driver to attain better lane-keeping performance. In comparison with the aforementioned literature, e.g., [7], [9], a pre-identified driver model is not necessary, and the accurate knowledge of the vehicle is no longer needed. The design procedure of our proposed controller relies on measurable data collected in real time from the human driver and his/her vehicle. In particular, only the driver's steering torque is required, leaving the internal states of the driver dynamics unmeasured. The main contributions of this paper are three-fold. First, by taking advantage of the state-space small-gain theory of interconnected systems [33], [34], the designed cooperative controller does not depend on the unmeasurable internal states of the driver. Second, by employing a data-driven learning-based approach, the shared steering controller is learned online from measurable data of the interconnected human-vehicle system, without the exact knowledge of the driver and the vehicle. Such a data-driven method provides more personalized service for the driver and improves the adaptivity of the cooperative controller for the vehicle. Third, compared to [24], a novel iterative learning strategy is introduced to solve the output regulation problem with non-vanishing signal caused by driver's steering command. More specifically, the driver generates non-zero steering torque into the vehicle along with the designed control input.

The rest of the paper is organized as follows. Section II describes the mathematical model of an interconnected system of the driver and the vehicle. Section III illustrates a model-based method to design an optimal cooperative controller for the driver in order to achieve the lane keeping. Section IV presents a data-driven approach to solve the optimal cooperative control problem in the presence of unknown driver and vehicle dynamics (e.g., unknown system parameters). Section V depicts computer-based numerical simulation results under different road conditions. Section VI gives the conclusion of this paper.

**Notations.** Throughout this paper,  $\mathbb{R}$ ,  $\mathbb{R}_+$ ,  $\mathbb{Z}_+$ , and  $\mathbb{C}$  denote the sets of real numbers, non-negative real numbers, non-negative integers, and complex numbers, respectively.  $\mathbb{C}^-$  stands for the open left-half complex plane.  $|\cdot|$  represents the Euclidean norm for vectors, or the induced matrix norm for matrices.  $\otimes$  indicates the Kronecker product.  $\text{vec}(A) = [a_1^T, a_2^T, \dots, a_m^T]^T$ , where  $a_i \in \mathbb{R}^n$  are the columns of  $A \in \mathbb{R}^{n \times m}$ . When  $m = n$ ,  $\sigma(A)$  is its complex spectrum.  $I_n$  represents the  $n \times n$  identity matrix.  $0_{n \times m}$  denotes the  $n \times m$  zero matrix. For a symmetric matrix  $P \in \mathbb{R}^{m \times m}$ ,  $\lambda_M(P)$  is the maximum eigenvalue of  $P$ ;  $\lambda_m(P)$  is the minimum eigenvalue of  $P$ ; and  $\text{vecs}(P) = [p_{11}, 2p_{12}, \dots, 2p_{1m}, p_{22}, 2p_{23}, \dots, 2p_{m-1,m}, p_{mm}]^T \in \mathbb{R}^{\frac{1}{2}m(m+1)}$ . For an arbitrary column vector  $v \in \mathbb{R}^n$ ,  $\text{vecv}(v) = [v_1^2, v_1v_2, \dots, v_1v_n, v_2^2, \dots, v_{n-1}v_n, v_n^2]^T \in \mathbb{R}^{\frac{1}{2}n(n+1)}$ .

## II. MATHEMATICAL MODELING FOR HUMAN-VEHICLE INTERACTION

In this section, the vehicle model and the human driver model are presented. Then, we combine them into the human-vehicle model as an interconnected system.

### A. Vehicle Lateral Dynamics

The vehicle model for steering control consists of the lateral vehicle dynamics, the steering column and the vision-position model for lane-keeping task. According to [12], [35], under the assumptions of small angles and constant longitudinal speed, it can be described by

$$\begin{aligned} \dot{x} &= Ax + B(u + T_d) + D\rho_i, \\ y &= Cx, \end{aligned} \quad (1)$$

where  $x = [v_y \ r_a \ \psi_L \ y_L \ \delta \ \dot{\delta}]^T$ ,  $y = y_c$ , and  $\psi_L = \psi_v - \psi_r$  as illustrated in Fig. 2. The matrices  $A$ ,  $B$ ,  $C$  and  $D$  are expressed as

$$\begin{aligned} A &= \begin{bmatrix} a_{11} & a_{12} & 0 & 0 & b_1 & 0 \\ a_{21} & a_{22} & 0 & 0 & b_2 & 0 \\ 0 & 1 & 0 & 0 & 0 & 0 \\ 1 & l_s & v_x & 0 & 0 & 0 \\ 0 & 0 & 0 & 0 & 0 & 1 \\ T_{s1} & T_{s2} & 0 & 0 & T_{s3} & T_{s4} \end{bmatrix}, B = \begin{bmatrix} 0 \\ 0 \\ 0 \\ 0 \\ 0 \\ \frac{1}{I_s R_s} \end{bmatrix}, \\ C &= [0 \ 0 \ -l_s \ 1 \ 0 \ 0], \\ D &= [0 \ 0 \ -v_x \ 0 \ 0 \ 0]^T, \end{aligned}$$

where

$$\begin{aligned} a_{11} &= -\frac{2(C_f + C_r)}{mv_x}, \quad a_{12} = \frac{2(C_r l_r - C_f l_f)}{mv_x} - v_x, \\ a_{21} &= \frac{2(C_r l_r - C_f l_f)}{I_z v_x}, \quad a_{22} = \frac{-2(C_f l_f^2 + C_r l_r^2)}{I_z v_x}, \\ b_1 &= \frac{2C_f}{m}, \quad b_2 = \frac{2C_f l_f}{I_z}, \quad T_{s1} = \frac{2C_f \eta_t}{I_s R_s^2 v_x}, \\ T_{s2} &= \frac{2C_f l_f \eta_t}{I_s R_s^2 v_x}, \quad T_{s3} = \frac{-2C_f \eta_t}{I_s R_s^2}, \quad T_{s4} = -\frac{B_s}{I_s}. \end{aligned}$$

In (1), the model is expressed by a constant curvature  $\rho_i$ , where subscript  $i$  indicates the index of road segment. Practically, the road curvature can be approximated by piecewise constant functions as in [7], [9], [12].

### B. Human Driver Model

In this paper, we consider the two-point visual driver model developed in [17], which has been validated to demonstrate satisfactory model accuracy for lane keeping task [36], [37].

The visual input to the human driver consists of two regions: (1) near point; (2) far point. These two visual regions represent driver's compensatory and anticipatory driving behavior [17], respectively. The information provided by these two points can be expressed by two visual angles  $\theta_{near}$  and  $\theta_{far}$  [36], where  $\theta_{near} = \psi_L + y_L/l_s$  and  $\theta_{far} = D_{far}\rho_i$ . When the vehicle approaches a curving road,  $D_{far}$  is a constant in the

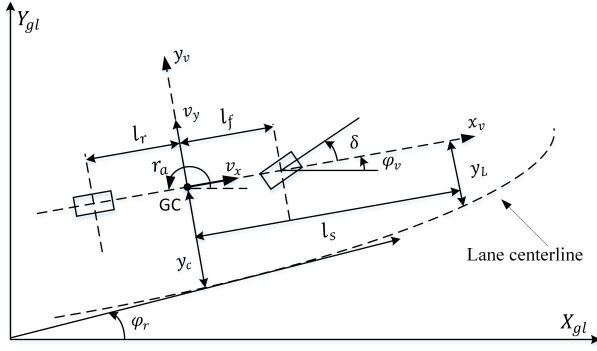


Fig. 2. Vehicle model illustration

range of 10 – 20 [m] according to the road curvature [38]. Thus, we can see that the driver's compensatory action is mostly based on the information in front of the vehicle, and the anticipatory response depends on the road aspects, i.e., the curvature. After processing the visual information, the driver adjusts his/her steering torque through the steering wheel to achieve lane keeping control of the vehicle, i.e., following the lane centerline. Based on this process, the driver model can take the following state-space form [36]:

$$\begin{aligned} \dot{\zeta} &= A_d \zeta + B_d x + D_d \rho_i, \\ T_d &= C_d \zeta, \end{aligned} \quad (2)$$

where  $\zeta = [\zeta_1 \quad \zeta_2]^T$ . The matrices are given as follows:

$$A_d = \begin{bmatrix} a_{11d} & 0 \\ a_{21d} & a_{22d} \end{bmatrix}, B_d = \begin{bmatrix} 0 & 0 & b_{11d} & \frac{b_{11d}}{l_s} & 0 & 0 \\ 0 & 0 & b_{21d} & \frac{b_{21d}}{l_s} & 0 & 0 \end{bmatrix},$$

$$C_d = [0 \quad 1], D_d = \begin{bmatrix} 0 \\ b_{22d} D_{far} \end{bmatrix},$$

where  $a_{11d} = -\frac{1}{T_I}$ ,  $a_{21d} = \frac{1}{T_N T_I}$ ,  $a_{22d} = -\frac{1}{T_N}$ ,  $b_{11d} = -\frac{(T_I - T_L) K_c}{T_I}$ ,  $b_{21d} = -\frac{T_L K_c}{T_I T_N}$ ,  $b_{22d} = \frac{K_a}{T_N}$ . It is observed that  $A_d$  is a stable matrix, i.e., both eigenvalues of  $A_d$  have negative real parts [36].

Combining (1) and (2), we obtain an interconnected system model that captures the interaction between the driver and the vehicle.

### III. MODEL-BASED CONTROL DESIGN FOR SHARED STEERING

In this section, we present some preliminary results that are necessary for the shared steering controller design.

#### A. Output Regulation Problem with Partial-state Feedback

Recall that the goal of achieving lane keeping is to design a feedback controller to force the output  $y$  of system (1) to zero, that is,  $\lim_{t \rightarrow \infty} y(t) = 0$ . The output regulation problem, also called servomechanism problem, intends to design a feedback controller to achieve asymptotic tracking with disturbance rejection for a reference input while preserving the closed-loop stability [39]. Thus, output regulation is a powerful tool

to accomplish the goal of lane keeping, where the reference trajectory is given by the road.

It is worth noting that this control task is challenging, because the driver states  $\zeta$  are not all measurable and thus are unavailable to the designer. In other words, in the absence of full-state information, a partial-state feedback design algorithm is needed for the desired control objective.

**Theorem 1.** Considering (1) and (2), if a control gain  $K = [0_{1 \times 2} \quad K] \in \mathbb{R}^8$  satisfies that  $\sigma(A - BK) \in \mathbb{C}^-$ , where

$$A = \begin{bmatrix} A_d & B_d \\ BC_d & A \end{bmatrix}, B = \begin{bmatrix} 0_{2 \times 1} \\ B \end{bmatrix}, \quad (3)$$

and the controller takes the following form

$$u = -Kx + (U^* + KX^*)\rho_i \quad (4)$$

where  $X^* \in \mathbb{R}^6$ ,  $U^* \in \mathbb{R}$  and  $Z^* \in \mathbb{R}^2$  satisfy the following regulator equations

$$0 = A_d Z^* + B_d X^* + D_d, \quad (5)$$

$$0 = AX^* + BU^* + D + BC_d Z^*, \quad (6)$$

$$0 = CX^*, \quad (7)$$

then the asymptotic convergence of the lane-keeping error is achieved, i.e.,  $\lim_{t \rightarrow \infty} y(t) = 0$ .

*Proof.* Define  $\bar{x} = x - X^* \rho_i$ ,  $\bar{u} = u - U^* \rho_i$ , and  $\bar{\zeta} = \zeta - Z^* \rho_i$ . Using (5)-(7), the error dynamics can be formulated as follows

$$\dot{\bar{\zeta}} = A_d \bar{\zeta} + B_d \bar{x}, \quad (8)$$

$$\dot{\bar{x}} = A \bar{x} + B(\bar{u} + C_d \bar{\zeta}), \quad (9)$$

$$y = C \bar{x}. \quad (10)$$

Since we have  $\bar{u} = -K \bar{x}$  and  $\sigma(A - BK) \in \mathbb{C}^-$ , the closed-loop error system (8)-(10) is stable, i.e.,  $\lim_{t \rightarrow \infty} \bar{x}(t) = 0$ . Therefore,  $\lim_{t \rightarrow \infty} y(t) = 0$ .  $\square$

Theorem 1 provides a potential design procedure to achieve shared control between the driver and the vehicle. However, it is noted that the transient performance of the closed-loop system with the controller (4) is determined by the parameterization of  $K$ , and is not guaranteed. In the following subsection, an optimal control framework for cooperative steering is introduced, which aims to obtain improved performance.

#### B. Linear Quadratic Regulator (LQR) and Robustness Analysis

Now, we present the strategy to find a control gain  $K$  satisfying the condition in Theorem 1. In order to attain satisfactory transient performance during lane-keeping task, we introduce the following optimal control problem widely known as the LQR problem:

$$\begin{aligned} & \underset{\bar{u}}{\text{minimize}} && \int_0^\infty [\bar{x}^T Q \bar{x} + r \bar{u}^2] dt \\ & \text{subject to} && \dot{\bar{x}} = A \bar{x} + B \bar{u}, \\ & && y = C \bar{x}, \end{aligned}$$

where  $Q = Q^T \geq 0$ ,  $r > 0$  and  $(A, \sqrt{Q})$  is observable. Note that the driver's input is omitted here, since the performance index is defined for infinite horizon. By removing the driver's input, the optimality can be guaranteed when the fully autonomous mode is considered. In the presence of the driver's input, stability/robustness can be ensured for the interconnected system of the driver and the vehicle, as we will present later.

By linear optimal control theory [40], the optimal controller  $\bar{u}^* = -K^*\bar{x}$  solving the above LQR problem is determined by

$$K^* = \frac{1}{r}B^T P^*, \quad (11)$$

where  $P^* = (P^*)^T > 0$  is the unique solution to the algebraic Riccati equation

$$A^T P + P A + Q - \frac{1}{r} P B B^T P = 0. \quad (12)$$

Next, we consider the error dynamics (8)-(10), where driver's behavior is taken into consideration. The following result introduces a property of the driver model (2).

**Lemma 1.** *Let  $c_1 = |C_d|^2$ . Then, there exist a Lyapunov function  $W(\bar{\zeta}) = \bar{\zeta}^T M \bar{\zeta}$  where  $M = M^T > 0$  is the unique solution to the Lyapunov equation*

$$A_d^T M + M A_d = -2c_1 I_2, \quad (13)$$

and a constant  $c_2 \geq \frac{1}{c_1} \lambda_M(B_d^T M M B_d)$ , such that

$$\dot{W} \leq -c_1 |\bar{\zeta}|^2 + c_2 |\bar{x}|^2. \quad (14)$$

*Proof.* See the Appendix.

In practice, the accurate knowledge of matrices  $A_d$  and  $B_d$  is difficult to acquire. Here, instead of assuming the perfect model for driver, we only assume that the gain  $c_2$  from  $\bar{x}$  to  $\bar{\zeta}$  is known.

Next, the stabilization problem of (8)-(10) can be studied using the small-gain theorem [33], [41]; see the Appendix for a short review. The following theorem gives the solution to obtain an optimal controller that forces the lane keeping error  $y$  to zero.

**Theorem 2.** *Let  $\bar{u}^* = -K^*\bar{x}$  be the optimal controller obtained by (11) with the symmetric matrix  $Q \geq \gamma_x I_6$  for  $\gamma_x > c_2$ , and  $r = 1$ . Then, the error system (8)-(10) is stabilized, i.e.,  $\sigma(A - BK^*) \in \mathbb{C}^-$  with  $K^* = [0_{1 \times 2} \quad K^*] \in \mathbb{R}^{1 \times 8}$ . Furthermore,  $\lim_{t \rightarrow \infty} y = 0$ .*

*Proof.* Consider  $V(\bar{x}) = \bar{x}^T P^* \bar{x}$ . Differentiating  $V(\bar{x})$ , we have

$$\begin{aligned} \dot{V} &= \bar{x}^T [(A - BK^*)^T P^* + P^* (A - BK^*)] \bar{x} \\ &\quad + 2\bar{x}^T P^* B C_d \bar{\zeta} \\ &= -\bar{x}^T (Q + P^* B B^T P^*) \bar{x} + 2\bar{x}^T P^* B C_d \bar{\zeta} \\ &\leq -\bar{x}^T Q \bar{x} - |C_d \bar{\zeta} - B^T P^* \bar{x}|^2 + c_1 |\bar{\zeta}|^2 \\ &\leq -\gamma_x |\bar{x}|^2 + c_1 |\bar{\zeta}|^2 \end{aligned} \quad (15)$$

From (15), it can be derived that the  $\mathcal{L}_2$ -gain [41] of the vehicle-road system (9) and (10) is  $\sqrt{\frac{c_1}{\gamma_x}}$ . Similarly, (14)

implies that the  $\mathcal{L}_2$ -gain of the driver system (8) is  $\sqrt{\frac{c_2}{c_1}}$ . Since  $\sqrt{\frac{c_1}{\gamma_x}} \cdot \sqrt{\frac{c_2}{c_1}} < 1$ , the stability of the interconnected system (8)-(10) follows readily from the small-gain theorem [42]. Indeed, considering  $V_1(\bar{x}, \bar{\zeta}) = V(\bar{x}) + W(\bar{\zeta})$ , we have  $\dot{V}_1 \leq -(\gamma_x - c_2) |\bar{x}|^2 \leq 0$ .  $\square$

**Remark 1.** *The upper bound of  $c_2$  can be estimated when a large amount of historical driver data are collected, such as the data of drivers from different age groups and from different countries. We can choose  $Q$ , when the upper bound of  $c_2$  is determined.*

**Remark 2.** *It is of interest to note that the stabilizing control gain  $K^*$  does not depend on the unmeasurable states  $\zeta$  of the driver.*

### C. Optimality Analysis

As we mentioned in the previous subsection, the control law  $K^*$  is optimal in the case of fully autonomous mode. Now, we present an optimality analysis when the optimal controller  $K^*$  is applied to the vehicle with a human driver in the loop.

As a result of Theorem 2, the error state  $\bar{x}$  and the error steering input  $\bar{u}$  are convergent, and thus there exist positive constants  $\alpha_{\bar{x}}$ ,  $\beta_{\bar{x}}$  and  $\beta_{\bar{u}}$  such that

$$|\bar{x}(t)| \leq |\bar{x}(0)| \beta_{\bar{x}} e^{-\alpha_{\bar{x}} t}, \quad (16)$$

$$|\bar{u}(t)| \leq |\bar{u}(0)| \beta_{\bar{u}} e^{-\alpha_{\bar{x}} t}. \quad (17)$$

In particular, the constants  $\alpha_{\bar{x}}$ ,  $\beta_{\bar{x}}$  and  $\beta_{\bar{u}}$  are determined by the eigenvalues of the closed-loop driver-vehicle system, i.e.,  $\sigma(A - BK^*)$ . Let  $J^\oplus$  denote the performance of the optimal controller  $K^*$  in the presence of a human driver. Thus, from (16)-(17), we have

$$\begin{aligned} J^\oplus &= \int_0^\infty [\bar{x}^T(t) Q \bar{x}(t) + r \bar{u}^2(t)] dt \\ &\leq \frac{\lambda_M(Q) \beta_{\bar{x}}^2 + r \beta_{\bar{u}}^2}{2\alpha_{\bar{x}}} |\bar{x}(0)|^2. \end{aligned} \quad (18)$$

On the other hand, when there is no driver's input to the vehicle, the optimal performance is well known as  $J^* = \bar{x}^T(0) P^* \bar{x}(0)$ . Hence, an upper bound of the performance difference caused by the human driver's steering input can be quantified as follows

$$J^\oplus \leq \mu^{-1} J^*, \quad (19)$$

where  $\mu = \frac{2\alpha_{\bar{x}} \lambda_m(P^*)}{\lambda_M(Q) \beta_{\bar{x}}^2 + r \beta_{\bar{u}}^2}$ .

### D. A Model-based Algorithm to Find $K^*$

The following technical result is reviewed to give an algorithm to find  $K^*$  in Theorem 2.

**Lemma 2.** (*[43]*) *Let  $K_0$  be an initial stabilizing controller such that  $\sigma(A - BK_0) \in \mathbb{C}^-$ . For an integer  $j \geq 1$ , let  $P_j = P_j^T > 0$  be the solution to the following Lyapunov equation*

$$(A - BK_j)^T P_j + P_j (A - BK_j) + Q + r K_j^T K_j = 0, \quad (20)$$

where  $K_j$  is decided by

$$K_j = \frac{1}{r} B^T P_{j-1}. \quad (21)$$

Then, the following properties hold:

- 1)  $\sigma(A - BK_j) \in \mathbb{C}^-$ ,
- 2)  $P^* \leq P_j \leq P_{j-1}$ ,
- 3)  $\lim_{j \rightarrow \infty} K_j = K^*$ ,  $\lim_{j \rightarrow \infty} P_j = P^*$ ,

where  $K^*$  and  $P^*$  are defined in (11) and (12).

Hitherto, the stabilizing control gain  $K^*$  and the solutions  $X^*$ ,  $U^*$  and  $Z^*$  to the modified regulator equations (5)-(7) are still dependent on the known parameters of the driver ( $A_d, B_d$ ) and the vehicle ( $A, B$ ). We shall overcome this obstacle by a data-driven approach presented in the next section.

#### IV. DATA-DRIVEN DESIGN APPROACH FOR STEERING ASSISTANCE

In this section, an iterative learning framework is first proposed to solve the modified regulator equations (5)-(7) with unknown driver model matrices  $A_d$  and  $B_d$ . Then, we present a data-driven learning strategy to approximate the unknown optimal values  $K^*$ ,  $X^*$  and  $U^*$ , even when the vehicle system matrices  $A$  and  $B$  are also unknown.

##### A. Solving the Modified Regulator Equations with Unknown Driver Model

Here, we propose the following iterative learning framework to solve (5)-(7) with driver's torque  $T_d$  being measurable, under the condition that the human driver system matrices  $A_d$  and  $B_d$  are unknown.

By means of the controllable canonical form of  $(A, B)$ , we have the following result.

**Lemma 3.** Let  $K = [k_1 \ k_2 \ k_3 \ k_4 \ k_5 \ k_6]$  be a stabilizing control gain for the vehicle system, i.e.,  $\sigma(A - BK) \in \mathbb{C}^-$ . Then,  $k_4 > 0$ .

*Proof.* See the Appendix.

In this subsection, assume that an approximate optimal controller  $K_{j^*}$  is given by Lemma 2, where  $j^*$  is the iteration index when Kleinman's algorithm is stopped, i.e., the difference between  $K_{j^*}$  and  $K^*$  is small enough. Since  $\sigma(A - BK_{j^*}) \in \mathbb{C}^-$ , we have  $k_{j^*,4} > 0$ .

Now, we can start our learning/adaptation as follows. First, we collect the driver's torque  $T_0 = C_d \mathcal{Z}_0 \rho_0$  on any constant-curvature part of a road, where  $\mathcal{Z}_0 \in \mathbb{R}^2$  and  $\mathcal{Z}_0 \rho_0$  is the steady state of the driver with  $u_0 = 0$ , i.e., without any steering assistance.

Then, on the  $i$ -th segment of the road, we let the controller  $u_i = -K_{j^*} x + (\hat{U}_i + K_{j^*} \hat{\mathcal{X}}) \rho_i$  help the driver complete lane keeping, where  $\hat{\mathcal{X}}$  and  $\hat{U}_i$  satisfy

$$0 = A \hat{\mathcal{X}} + B \hat{U}_i + D + \frac{B}{\rho_{i-1}} T_{i-1}, \quad (22)$$

$$0 = C \hat{\mathcal{X}}, \quad (23)$$

where  $T_{i-1} = C_d \mathcal{Z}_{i-1} \rho_{i-1}$  is the driver's applied torque,  $\mathcal{Z}_{i-1} \in \mathbb{R}^2$  and  $\mathcal{Z}_{i-1} \rho_{i-1}$  is the steady state of the driver with  $u_{i-1}$ .

Next, we study the steady state of both human driver (2) and the vehicle (1), when the updated controller  $u_i$  is applied. Define  $\tilde{\zeta}_i = \zeta - \mathcal{Z}_i \rho_i$  and  $\tilde{x}_i = x - \mathcal{X}_i \rho_i$ , with  $\mathcal{Z}_i \in \mathbb{R}^2$  and  $\mathcal{X}_i \in \mathbb{R}^6$ . Then, from (2) we have

$$\dot{\tilde{\zeta}}_i = A_d \tilde{\zeta}_i + B_d \tilde{x}_i + (A_d \mathcal{Z}_i + B_d \mathcal{X}_i + D_d) \rho_i \quad (24)$$

With (1), we have

$$\begin{aligned} \dot{\tilde{x}}_i &= A x_i + B(u_i + C_d \zeta) + D \rho_i \\ &= (A - BK_{j^*}) \tilde{x}_i + BC_d \tilde{\zeta}_i \\ &\quad + [(A - BK_{j^*})(\mathcal{X}_i - \hat{\mathcal{X}}) + BC_d(\mathcal{Z}_i - \mathcal{Z}_{i-1})] \rho_i. \end{aligned}$$

Thus, for the steady state, it follows that

$$0 = A_d \mathcal{Z}_i + B_d \mathcal{X}_i + D_d, \quad (25)$$

$$0 = (A - BK_{j^*})(\mathcal{X}_i - \hat{\mathcal{X}}) + BC_d(\mathcal{Z}_i - \mathcal{Z}_{i-1}), \quad (26)$$

$$T_i = C_d \mathcal{Z}_i \rho_i. \quad (27)$$

By MATLAB and Symbolic Math Toolbox [44], we are able to study the relationship between  $X^*$  and  $\hat{\mathcal{X}}$  as follows. Note that (22), (23) and (27) imply

$$\begin{bmatrix} A & B \\ C & 0 \end{bmatrix} \begin{bmatrix} \hat{\mathcal{X}} \\ \hat{U}_i \end{bmatrix} = \begin{bmatrix} -D \\ 0 \end{bmatrix} + \begin{bmatrix} -BC_d \\ 0 \end{bmatrix} \mathcal{Z}_{i-1}. \quad (28)$$

Likewise, (6) and (7) can be written into

$$\begin{bmatrix} A & B \\ C & 0 \end{bmatrix} \begin{bmatrix} X^* \\ U^* \end{bmatrix} = \begin{bmatrix} -D \\ 0 \end{bmatrix} + \begin{bmatrix} -BC_d \\ 0 \end{bmatrix} Z^*. \quad (29)$$

Then, it is checkable that

$$X^* = \hat{\mathcal{X}} = \text{diag}(1, 1, 1, 1, 1, 0) \begin{bmatrix} A & B \\ C & 0 \end{bmatrix}^{-1} \begin{bmatrix} -D \\ 0 \end{bmatrix}, \quad (30)$$

$$\text{since } \begin{bmatrix} A & B \\ C & 0 \end{bmatrix}^{-1} \begin{bmatrix} -BC_d \\ 0 \end{bmatrix} = \begin{bmatrix} 0_{6 \times 1} & 0_{6 \times 1} \\ 0 & -1 \end{bmatrix}.$$

**Remark 3.** From (30), it is remarked that  $X^* = \hat{\mathcal{X}}$  is independent of driver's steady state  $\mathcal{Z}_{i-1}$ , i.e., it only relies on the vehicle parameters in  $A$  and  $B$ .

Next, we explore the connection between the steady states  $\mathcal{Z}_i$  and  $\mathcal{Z}_{i-1}$ , i.e., the driver's adaptation of the cooperative controller  $u_i$ . Observe that (26) gives

$$\mathcal{X}_i = \hat{\mathcal{X}} - (A - BK_{j^*})^{-1} BC_d(\mathcal{Z}_i - \mathcal{Z}_{i-1}). \quad (31)$$

Then, putting (31) into (25), we obtain

$$\mathcal{Z}_i = F_1 \mathcal{Z}_{i-1} + F_2 \hat{\mathcal{X}} + L_1, \quad (32)$$

where  $G = B_d(A - BK_{j^*})^{-1} BC_d$ ,  $E = -(A_d - G)^{-1}$ ,  $F_1 = EG$ ,  $F_2 = EB_d$ ,  $L_1 = ED_d$ . It is verifiable that one of the eigenvalues of  $F_1$  is always zero, and the other one  $\mu_{F_1}$  is given by

$$\begin{aligned} \mu_{F_1} &= \frac{a_{11d} b_{21d} - a_{21d} b_{11d}}{a_{11d} b_{21d} - a_{21d} b_{11d} + a_{11d} a_{22d} k_{j^*,4} l_s} \\ &= \frac{K_c}{K_c + k_{j^*,4} l_s}. \end{aligned} \quad (33)$$

From Lemma 3, we have that both eigenvalues of  $F_1$  are in the unit disk, which implies that

$$\lim_{i \rightarrow \infty} |Z_i - Z_{i-1}| = 0. \quad (34)$$

In addition, (30) and (31) give that

$$\lim_{i \rightarrow \infty} \mathcal{X}_i = \widehat{\mathcal{X}} = X^*. \quad (35)$$

Further, from (25), we have

$$\lim_{i \rightarrow \infty} Z_i = Z^*, \quad (36)$$

since  $A_d$  is of full rank. Therefore, by (28), (29) and (36), the following holds

$$\lim_{i \rightarrow \infty} \widehat{U}_i = U^*. \quad (37)$$

**Remark 4.** By the iterative learning steps (22)-(23),  $X^*$  and  $U^*$  can be approximated without the accurate driver model  $A_d$  and  $B_d$ .

So far, we still rely on the exact knowledge of the vehicle system  $(A, B)$  to solve (22)-(23) and  $K_{j^*}$  for the shared controller design. Meanwhile, it is desirable to provide more personalized service for each driver when he/she is driving different vehicles, which requires that the parametric variations of the vehicle do not affect the steering performance. This necessity motivates the following data-driven methodology to design the steering assistance system.

### B. Data-driven RADP Method for Shared Steering Control with Unknown Vehicle Parameters

In this subsection, we apply an RADP framework to design a shared steering controller, i.e., to find the approximate values for  $K_{j^*}$ ,  $X^*$  and  $U^*$ , while the accurate knowledge of vehicle model matrices  $A$  and  $B$  is not available.

Now, we revisit the iterative learning framework of  $\widehat{\mathcal{X}}$  and  $\widehat{U}_i$  in (22) and (23) for  $i \geq 1$ , given driver's torque  $T_0$  at steady state. Motivated by [24], it is not difficult to see that  $\widehat{\mathcal{X}}$  can be expressed by

$$\widehat{\mathcal{X}} = Y^1 + \sum_{l=2}^6 \alpha^l Y^l \quad (38)$$

where  $Y^1 = 0_{6 \times 1}$ , and for  $l = 2, \dots, 6$ ,  $\alpha^l \in \mathbb{R}$  and  $Y^l \in \mathbb{R}^6$  such that  $CY^l = 0$ , i.e.,  $Y^l$  form the null space of  $C$ .

Here, an online data-driven learning method is proposed to find  $K^*$ ,  $\widehat{\mathcal{X}}$  and  $\widehat{U}_i$ . Let  $\bar{x}^l = x - Y^l \rho_i$ , for  $l = 1, \dots, 6$ . It follows that

$$\begin{aligned} \dot{\bar{x}}^l &= Ax + B(u + T_d) + D\rho_i \\ &= A_j \bar{x}^l + B(K_j \bar{x}^l + w) + (D + AY^l)\rho_i \end{aligned} \quad (39)$$

where  $A_j = A - BK_j$  and  $w = u + T_d$ . Then, we have

$$\begin{aligned} & [\bar{x}^l(t + \delta t)]^T P_j \bar{x}^l(t + \delta t) - [\bar{x}^l(t)]^T P_j \bar{x}^l(t) \\ &= \int_t^{t+\delta t} [(\bar{x}^l)^T (A_j^T P_j + P_j A_j) \bar{x}^l + 2(K_j \bar{x}^l + w) B^T P_j \bar{x}^l \\ &\quad + 2\rho_i (D + AY^l)^T P_j \bar{x}^l] d\tau \\ &= - \int_t^{t+\delta t} (\bar{x}^l)^T (Q + rK_j^T K_j) \bar{x}^l d\tau \\ &\quad + 2 \int_t^{t+\delta t} r(w + K_j \bar{x}^l) K_{j+1} \bar{x}^l d\tau \\ &\quad + 2 \int_t^{t+\delta t} \rho_i (D + AY^l)^T P_j \bar{x}^l d\tau. \end{aligned} \quad (40)$$

Following Kronecker product representation, we have

$$\begin{aligned} (\bar{x}^l)^T (Q + rK_j^T K_j) \bar{x}^l &= [(\bar{x}^l)^T \otimes (\bar{x}^l)^T] \text{vec}(Q + rK_j^T K_j), \\ \rho_i (D + AY^l)^T P_j \bar{x}^l &= [(\bar{x}^l)^T \otimes \rho_i] \text{vec}((D + AY^l)^T P_j), \\ r(w + K_j \bar{x}^l) K_{j+1} \bar{x}^l &= \\ &= [((\bar{x}^l)^T \otimes (\bar{x}^l)^T) (I_6 \otimes rK_j^T) + r((\bar{x}^l)^T \otimes w) I_6] \text{vec}(K_{j+1}). \end{aligned}$$

Further, for positive integer  $s$ , we define

$$\begin{aligned} \delta_{\bar{x}^l \bar{x}^l} &= [\text{vecv}(\bar{x}^l(t_1)) - \text{vecv}(\bar{x}^l(t_0)), \text{vecv}(\bar{x}^l(t_2)) - \\ &\quad \text{vecv}(\bar{x}^l(t_1)), \dots, \text{vecv}(\bar{x}^l(t_s)) - \text{vecv}(\bar{x}^l(t_{s-1}))]^T, \\ \Gamma_{\bar{x}^l \bar{x}^l} &= [\int_{t_0}^{t_1} \bar{x}^l \otimes \bar{x}^l d\tau, \int_{t_1}^{t_2} \bar{x}^l \otimes \bar{x}^l d\tau, \dots, \int_{t_{s-1}}^{t_s} \bar{x}^l \otimes \bar{x}^l d\tau]^T, \\ \Gamma_{\bar{x}^l w} &= [\int_{t_0}^{t_1} \bar{x}^l \otimes w d\tau, \int_{t_1}^{t_2} \bar{x}^l \otimes w d\tau, \dots, \int_{t_{s-1}}^{t_s} \bar{x}^l \otimes w d\tau]^T, \\ \Gamma_{\bar{x}^l \rho_i} &= [\int_{t_0}^{t_1} \bar{x}^l \otimes \rho_i d\tau, \int_{t_1}^{t_2} \bar{x}^l \otimes \rho_i d\tau, \dots, \int_{t_{s-1}}^{t_s} \bar{x}^l \otimes \rho_i d\tau]^T, \end{aligned}$$

where  $t_0 < t_1 < \dots < t_s$  are time instants. Thus, (40) can be written into the following matrix equation

$$\Psi_j^l \begin{bmatrix} \text{vecs}(P_j) \\ \text{vec}(K_{j+1}) \\ \text{vec}((D + AY^l)^T P_j) \end{bmatrix} = \Phi_j^l, \quad (41)$$

where

$$\Psi_j^l = [\delta_{\bar{x}^l \bar{x}^l}, -2\Gamma_{\bar{x}^l \bar{x}^l} (I_6 \otimes rK_j^T) - 2\Gamma_{\bar{x}^l w} (rI_6), -2\Gamma_{\bar{x}^l \rho_i}], \quad (42)$$

$$\Phi_j^l = \Gamma_{\bar{x}^l \bar{x}^l} \text{vec}(Q + rK_j^T K_j). \quad (43)$$

**Assumption 1.** For  $l = 1, \dots, 6$  and  $j \in \mathbb{Z}_+$ , there exists a positive integer  $s^*$  such that for all  $s > s^*$  and for any  $t_0 < t_1 < \dots < t_s$ ,  $\Psi_j^l$  has full column rank.

**Remark 5.** To make Assumption 1 satisfied, an exploration noise  $\xi$  is introduced. In this paper, we choose  $\xi$  by adding sinusoidal functions with different frequencies as in [24], [25].

Under Assumption 1, (41) can be solved by the least-squares method as follows

$$\begin{bmatrix} \text{vecs}(P_j) \\ \text{vec}(K_{j+1}) \\ \text{vec}((D + AY^l)^T P_j) \end{bmatrix} = [(\Psi_j^l)^T \Psi_j^l]^{-1} (\Psi_j^l)^T \Phi_j^l. \quad (44)$$

Observe that  $D$  can be computed, since  $Y^1 = 0$ . Also,  $B$  can be estimated by  $B = rP_j^{-1} K_{j+1}^T$  and  $AY^l$  can be determined

for  $l = 2, \dots, 6$ . Thus, from (22) and (38),  $\hat{U}_i$  and the sequence  $\alpha^2, \dots, \alpha^6$  are solved by

$$\mathcal{S}(Y) + B\hat{U}_i = -(D + \frac{B}{\rho_{i-1}}T_{i-1}), \quad (45)$$

where  $\mathcal{S}(Y) = \sum_{l=2}^6 \alpha^l AY^l$ . Accordingly,  $\hat{\mathcal{X}}$  can be settled by (38).

The final algorithm for designing the data-driven shared steering controller is summarized as follows.

---

**Algorithm 1** Data-driven Shared Steering Control
 

---

- 1: Collect driver's  $T_0$  on the part of the road with curvature  $\rho_0$  when there is no steering assistance.
  - 2: Select  $K_0$  satisfying  $\sigma(A - BK_0) \in \mathcal{C}^-$ . Choose the weighting parameters  $Q = Q^T \geq c_2 I_6$  and  $r = 1$ . Let  $Y^1 = 0_{6 \times 1}$  and compute  $Y^l$  for  $l = 2, \dots, 6$ .  $j \leftarrow 0$ .  $i \leftarrow 1$ .
  - 3: **repeat**
  - 4: Apply an exploratory steering assistance:  $u = \xi$ .
  - 5: **for**  $l = 1$  **to** 6:
  - 6: Compute  $\Psi_j^l$  and  $\Phi_j^l$  from (42) and (43)
  - 7: **end for**
  - 8: **until** Assumption 1 is satisfied.
  - 9: Solve  $P_j$  and  $K_{j+1}$  from (44)
  - 10: **repeat**
  - 11:  $j \leftarrow j + 1$
  - 12: Update  $P_j$  and  $K_{j+1}$  from (44)
  - 13: **until**  $|P_j - P_{j-1}| < \gamma$
  - 14:  $j^* \leftarrow j$ .
  - 15: Find  $AY^l$  for  $l = 2, \dots, 6$  from (44). Solve  $\alpha^2, \dots, \alpha^6$ ,  $\mathcal{S}(Y)$  and  $\hat{U}_1$  from (45). Obtain  $\hat{\mathcal{X}}$  from (38).
  - 16: **repeat**
  - 17: **repeat**
  - 18: Apply  $u_i = -K_{j^*}x + (\hat{U}_i + K_{j^*}\hat{\mathcal{X}})\rho_i$
  - 19: **until** the  $i$ -th road segment is finished.
  - 20:  $i \leftarrow i + 1$ .
  - 21: Update  $\hat{U}_i$  from (45)
  - 22: **until**  $|\hat{U}_i - \hat{U}_{i-1}| < \epsilon$
  - 23:  $\hat{U}_{i^*} \leftarrow \hat{U}_i$ .
  - 24: The optimal controller  $u = -K_{j^*}x + (\hat{U}_{i^*} + K_{j^*}\hat{\mathcal{X}})\rho_i$ .
- 

**Remark 6.** Algorithm 1 is proposed for a fixed scenario, where the unknown parameters of the driver and the vehicle are constant during learning and application phase. When the parameters change, the algorithm is restarted so that the learned shared controller can adapt to the new scenario, such as a new driver-vehicle system with changed parameters.

**Theorem 3.** Under Assumption 1, the obtained sequences  $\{P_j\}_{j=0}^\infty$  and  $\{K_j\}_{j=1}^\infty$  from (44) satisfy

$$\lim_{j \rightarrow \infty} P_j = P^*, \quad \lim_{j \rightarrow \infty} K_j = K^*.$$

*Proof.* See the Appendix.

Next, we present the main result of this paper on the cooperative steering problem for semi-autonomous vehicles.

**Theorem 4.** Considering the vehicle system (1) and the driver model (2), let the shared steering controller  $u = -K_{j^*}x +$

$(\hat{U}_{i^*} + K_{j^*}\hat{\mathcal{X}})\rho_i$  be the result obtained from Algorithm 1. Then, we have the lane-keeping error converge to zero, i.e.,  $\lim_{t \rightarrow \infty} y(t) = 0$ .

*Proof.* See the Appendix.

**Remark 7.** To avoid the misuse of the proposed algorithm, i.e., the driver completely releases the control to the shared controller, we need to constantly measure driver's steering torque for safety. When the driver's torque is not detected for a duration of time, an alert should be sent to the driver, such as an audio signal.

## V. NUMERICAL SIMULATIONS

TABLE I  
NUMERICAL VALUES IN SIMULATIONS

Parameters	Numerical Values	Parameters	Numerical Values
$l_f$	1.0065 [m]	$I_z$	2454 [kg.m <sup>2</sup> ]
$l_r$	1.4625 [m]	$I_s$	0.05 [kg.m <sup>2</sup> ]
$m$	1500 [kg]	$R_s$	16
$l_s$	5 [m]	$B_s$	5.73
$\eta_t$	0.185 [m]	$C_r$	56636 [N/rad]
$C_f$	47135 [N/rad]	$T_N$	0.1 [s]
$K_a$	30	$K_c$	35
$T_I$	0.3 [s]	$T_L$	3 [s]

Several numerical simulations are conducted to demonstrate the efficacy of our proposed algorithm. The velocity  $v_x$  is fixed at 15 [m/s]. First, the driver controls the vehicle, without any steering assistance ( $u_0 = 0$ ), on the road segment where the curvature  $\rho_0 = 0.005$ . It is observed that the driver's torque at steady state is:  $T_0 = 8.12$  [N · m]. The other parameters are presented in Table I. We have  $K_0 = [10 \ 25 \ 100 \ 10 \ 1 \ 0.1]$ , and choose  $Y^l$  for  $l = 2, \dots, 6$  as follows

$$Y^2 = \begin{bmatrix} 0 \\ 0 \\ -1 \\ -5 \\ 0 \\ 0 \end{bmatrix}, Y^3 = \begin{bmatrix} 1 \\ 0 \\ 0 \\ 0 \\ 0 \\ 0 \end{bmatrix}, Y^4 = \begin{bmatrix} 0 \\ 1 \\ 0 \\ 0 \\ 0 \\ 0 \end{bmatrix}, Y^5 = \begin{bmatrix} 0 \\ 0 \\ 0 \\ 0 \\ 1 \\ 0 \end{bmatrix}, Y^6 = \begin{bmatrix} 0 \\ 0 \\ 0 \\ 0 \\ 0 \\ 1 \end{bmatrix},$$

which satisfy that  $CY^l = 0$ . Set  $r = 1$ . We will compare the performance with 3 different  $Q$  values, where  $Q^{(1)} = 100I_6$ ,  $Q^{(2)} = 500I_6$  and  $Q^{(3)} = 10000I_6$ . By the chosen weighting parameters, the theoretical optimal controllers can be solved by (11)-(12), and are characterized by  $K^{(1)*} = [12.05 \ 13.62 \ 143.59 \ 10.00 \ 14.39 \ 1.33]$ ,  $K^{(2)*} = [18.02 \ 20.43 \ 187.18 \ 22.36 \ 22.28 \ 1.98]$ ,  $K^{(3)*} = [38.20 \ 42.82 \ 194.56 \ 100.00 \ 51.92 \ 4.13]$ . Based on (5)-(7), we have  $X^* = [3.72 \ 15.00 \ -5.25 \ -26.24 \ 3.38 \ 0.00]^T$ ,  $U^* = 356.97$ .

We will evaluate our proposed steering assistance system on a test road. Fig. 3 shows the road curvature profile. In particular, the driver controls the vehicle with only exploratory assistance  $\epsilon$  in the first 2 seconds. According to line 3-8 in Algorithm 1, we collect the online state and input data of the vehicle until Assumption 1 is satisfied. That is, at time  $t = 2s$ ,

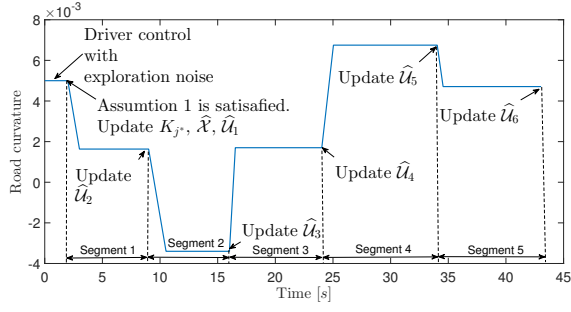


Fig. 3. Road curvature profile

we compute  $P_j$  and  $K_{j+1}$  as stated in line 9-15 for each  $Q$  value. After several iterations, we obtain three  $K_{j^*}$  as follows

$$K_6^{(1)} = [12.05 \ 13.62 \ 143.59 \ 10.00 \ 14.39 \ 1.33],$$

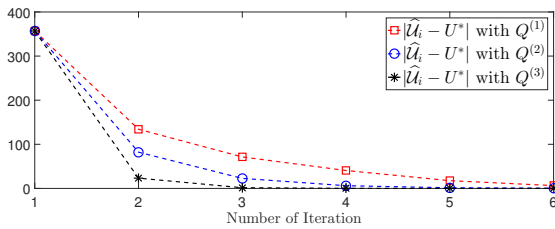
$$K_6^{(2)} = [18.02 \ 20.43 \ 187.18 \ 22.36 \ 22.28 \ 1.98],$$

$$K_{10}^{(3)} = [38.29 \ 42.82 \ 194.56 \ 100.00 \ 51.92 \ 4.13].$$

At the same time, we solve  $AY^l$  for  $l = 2, \dots, 6$  from (44). Next, the sequence  $\alpha^2, \dots, \alpha^6$  and  $\hat{U}_1$  are determined by (45). Thus, we obtain  $\hat{X} = [3.71 \ 15.00 \ -5.25 \ -26.24 \ 3.48 \ -0.62]^T$ ,  $\hat{U}_1 = 0.005$ . Then, we switch off the exploration noise, and update the learned shared controller to

$$u_i = -K_{j^*}x + (\hat{U}_i + K_{j^*}\hat{X})\rho_i,$$

which cooperates with the driver on the upcoming road segment  $i$ . Finally, the iterative learning steps begin as summarized in line 16-23, which are depicted in Fig. 3. More specifically, the update operation (45) on  $\hat{U}_i$  takes place whenever the vehicle is on a constant-curvature part of the road. Therefore, the learning process continues as the vehicle proceeds. In Fig. 4, we show that  $\hat{U}_i$  converges to its theoretical optimal value with different selected  $Q$  values.


 Fig. 4. Convergence of  $\hat{U}_i$  during driving with different chosen  $Q$  values

The lane-keeping error during the whole process is presented in Fig. 5, where the improved lane-keeping performance is self-evident with all 3 configurations. The undershoot and overshoot has been reduced compared to the driver-only scenario. In Fig. 6, we compare the driver's torque when there is no shared controller and his/her torque when different shared controllers are implemented. Driver's behaviors are influenced by the cooperative controllers, and larger  $Q$  value leads to larger undershoot and overshoot of driver's torque.

## VI. CONCLUSION

This paper studied a cooperative/shared steering control framework with human driver in the loop. Applying the state-

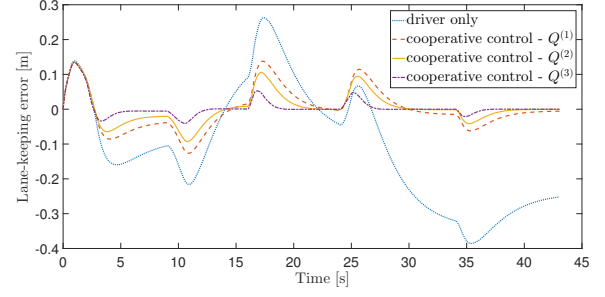
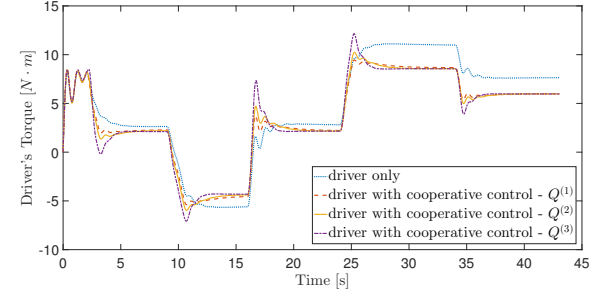

 Fig. 5. Lane-keeping performance comparison between driver and cooperative control strategies with different  $Q$  values


Fig. 6. Comparison of driver's torques

space small-gain theory to the interconnected system of both driver and vehicle, the designed shared controller does not rely on the information of the driver's internal states. Moreover, using RADP and output regulation theory, the steering controller collaborates with the driver to achieve desired lane-keeping performance, without the perfect knowledge of the driver and the vehicle. In particular, the shared steering controller can adapt to the driver's behavior by an online learning process. Rigorous analysis and proofs have been presented and the efficacy of our cooperative steering controller is validated through numerical simulations. Our future work will focus on the validation of our proposed algorithm to a hardware-in-the-loop driving simulator (e.g., CarSim) with real drivers and the shared control design for other driving tasks, such as collision avoidance and lane changing.

## APPENDIX A PROOF OF LEMMA 1

The existence and the uniqueness of  $M$  are guaranteed, since  $A_d$  is a stable matrix. Then, differentiating  $W(\zeta)$  with respect to time gives

$$\begin{aligned} \dot{W} &= \zeta^T (A_d^T M + M A_d) \zeta + \zeta^T M B_d \bar{x} + \bar{x}^T B_d^T M \zeta \\ &= -2c_1 |\zeta|^2 + \zeta^T M B_d \bar{x} + \bar{x}^T B_d^T M \zeta + c_1 \zeta^T \zeta - c_1 \zeta^T \zeta \\ &\quad + \frac{1}{c_1} \bar{x}^T B_d^T M M B_d \bar{x} - \frac{1}{c_1} \bar{x}^T B_d^T M M B_d \bar{x} \\ &= -c_1 |\zeta|^2 + \frac{1}{c_1} \bar{x}^T B_d^T M M B_d \bar{x} \\ &\quad - \left( \frac{1}{\sqrt{c_1}} M B_d \bar{x} - \sqrt{c_1} \zeta \right)^T \left( \frac{1}{\sqrt{c_1}} M B_d \bar{x} - \sqrt{c_1} \zeta \right) \\ &\leq -c_1 |\zeta|^2 + c_2 |\bar{x}|^2, \end{aligned}$$

where  $c_2 \geq \frac{1}{c_1} \lambda_M(B_d^T M M B_d)$ . The proof is completed.

#### APPENDIX B PROOF OF LEMMA 3

The controllability of the pair  $(A, B)$  implies that there exists a similarity transformation  $\mathcal{G}$ , such that  $\hat{A} = \mathcal{G}^{-1}A\mathcal{G}$ ,  $\hat{B} = \mathcal{G}^{-1}B$  are the controllable canonical form with controller  $\hat{K} = K\mathcal{G}$ . Let  $\hat{a}_{c6} = [\hat{a}_{c61} \ \hat{a}_{c62} \ \hat{a}_{c63} \ \hat{a}_{c64} \ \hat{a}_{c65} \ \hat{a}_{c66}]$  denote the last row of the closed-loop system  $\hat{A}_c = \hat{A} - \hat{B}\hat{K}$ . It can be checked that

$$\hat{a}_{c61} = \frac{k_4 C_f C_r (l_f + l_r)}{m I_z I_s R_s}.$$

Also, given stable poles  $\{p_1, \dots, p_6\} \subset \mathbb{C}^-$ ,  $\hat{a}_{c6}$  includes the coefficients of the closed-loop characteristic polynomial. Thus, we have  $\hat{a}_{c61} = \prod_{i=1}^6 p_i > 0$ . Therefore,  $k_4 > 0$ , which completes the proof.

#### APPENDIX C PROOF OF THEOREM 3

Given any stabilizing steering control law  $K_j$ , let  $P_j = P_j^T$  be the unique solution to (20), and  $\Lambda_j = (D + AY^l)^T P_j$ . Then, the updated steering controller  $K_{j+1}$  is determined by  $K_{j+1} = \frac{1}{r} B^T P_j$ . From (40), we have  $P_j$ ,  $K_{j+1}$  and  $\Lambda_j$  are the solutions to (44), which are solved by the measured data matrices  $\Psi_j^l$  and  $\Phi_j^l$ . In addition,  $P_j$ ,  $K_{j+1}$  and  $\Lambda_j$  are unique under Assumption 1. Hence, we have shown that (44) is equivalent to (20) and (21). Therefore, by Lemma 2, the convergence of  $P_j$  and  $K_j$  follows readily, which suggests that our data-driven algorithm is able to approximate the optimal control policy  $K^*$  that achieves desired steering performance.

#### APPENDIX D PROOF OF THEOREM 4

By Lemma 2 and Theorem 3, it follows that  $\sigma(A - BK_{j^*}) \in \mathbb{C}^-$ . Furthermore, we have  $\lim_{i \rightarrow \infty} \mathcal{Z}_i = Z^*$ ,  $\lim_{i \rightarrow \infty} \mathcal{X}_i = X^*$  and  $\lim_{i \rightarrow \infty} \mathcal{U}_i = U^*$ , which satisfy (5)-(7). Thus, we have the same error dynamics as (8)-(10). By Theorem 2, we have  $\lim_{t \rightarrow \infty} y(t) = 0$ . Thus, the proof is completed.

#### APPENDIX E REVIEW OF ISS AND SMALL-GAIN THEOREM

To make the paper self-contained, we briefly recall basic notions and results of input-to-state stability (ISS) and small-gain theorems, from the past literature (see, e.g., [33], [34], [45], [46]). Let  $\nabla V$  denote the gradient of a differentiable function  $V : \mathbb{R}^n \rightarrow \mathbb{R}$ .  $\|u\|$  stands for  $\sup_{t \geq 0} |u(t)|$ . A continuous function  $\gamma : \mathbb{R}_+ \rightarrow \mathbb{R}_+$  belongs to class  $\mathcal{K}$  if it is non-decreasing and  $\gamma(0) = 0$ . It is of class  $\mathcal{K}_\infty$  if additionally  $\gamma(s) \rightarrow \infty$  as  $s \rightarrow \infty$ . A function  $\beta : \mathbb{R}_+ \times \mathbb{R}_+ \rightarrow \mathbb{R}_+$  is of class  $\mathcal{KL}$  if for each fixed  $t$ , the function  $\beta(\cdot, t)$  is of class  $\mathcal{K}$ , and for each fixed  $s$ , the function  $\beta(s, \cdot)$  is non-increasing and tends to 0 at infinity. The notation  $\gamma_1 > \gamma_2$  means that  $\gamma_1(s) > \gamma_2(s)$ ,  $\forall s > 0$ , while  $\gamma_1 \circ \gamma_2$  denotes the composition of two functions, i.e., for all  $s \geq 0$ ,  $\gamma_1 \circ \gamma_2(s) = \gamma_1(\gamma_2(s))$ .

Consider the forced dynamical system of the form

$$\dot{x} = f(x, u), \quad (46)$$

where  $x \in \mathbb{R}^n$  is the state,  $u \in \mathbb{R}^m$  is the input, and  $f : \mathbb{R}^n \times \mathbb{R}^m \rightarrow \mathbb{R}^n$  is locally Lipschitz.

The ISS concept as reviewed below is a natural extension of Lyapunov stability from dynamical systems to control systems.

**Definition 1 ([45]):** The system (46) is said to be ISS with gain  $\gamma$  if, for all any measurable essentially bounded input  $u$  and any initial condition  $x(0)$ , the solution  $x(t)$  exists for every  $t \geq 0$  and satisfies

$$\|x(t)\| \leq \beta(\|x(0)\|, t) + \gamma(\|u\|), \quad (47)$$

where  $\beta$  is of class  $\mathcal{KL}$  and  $\gamma$  is of class  $\mathcal{K}$ .

**Definition 2 ([46]):** A continuously differentiable function  $V$  is said to be an ISS-Lyapunov function for the system (46) if  $V$  is positive definite and proper, and satisfies the following implication:

$$\|x\| \geq \chi(\|u\|) \Rightarrow \nabla V(x)^T f(x, u) \leq -\kappa(\|x\|), \quad (48)$$

where  $\kappa$  is positive definite and  $\chi$  is of class  $\mathcal{K}$ .

**Remark 8.** As it is well-known, an ISS system is internally globally asymptotically stable at the origin when  $u = 0$ , and is externally bounded-input bounded-state stable when  $u \neq 0$ . However, for nonlinear systems, the converse may not be true.

Then, consider an interconnected system described by

$$\dot{x}_1 = f_1(x_1, x_2, v), \quad (49)$$

$$\dot{x}_2 = f_2(x_1, x_2, v), \quad (50)$$

where, for each  $i = 1, 2$ ,  $x_i \in \mathbb{R}^{n_i}$ ,  $v \in \mathbb{R}^{n_v}$  and  $f_i : \mathbb{R}^{n_1} \times \mathbb{R}^{n_2} \times \mathbb{R}^{n_v} \rightarrow \mathbb{R}^{n_i}$  is locally Lipschitz, .

**Assumption 2.** For each  $i = 1, 2$ , there exists an ISS-Lyapunov function  $V_i$  for the  $x_i$  subsystem such that the following hold:

- 1) there exist functions  $\alpha_i, \bar{\alpha}_i \in \mathcal{K}_\infty$ , such that

$$\alpha_i(\|x_i\|) \leq V_i(x_i) \leq \bar{\alpha}_i(\|x_i\|) \quad \forall x_i \in \mathbb{R}^{n_i}; \quad (51)$$

- 2) there exist class  $\mathcal{K}$  functions  $\chi_i$  and  $\gamma_i$  and a class  $\mathcal{K}_\infty$  function  $\alpha_i$ , such that

$$\nabla V_1(x_1)^T f_1(x_1, x_2, v) \leq -\alpha_1(V_1(x_1)) \quad (52)$$

if  $V_1(x_1) \geq \max\{\chi_1(V_2(x_2)), \gamma_1(\|v\|)\}$ , and

$$\nabla V_2(x_2)^T f_2(x_1, x_2, v) \leq -\alpha_2(V_2(x_2)) \quad (53)$$

if  $V_2(x_2) \geq \max\{\chi_2(V_1(x_1)), \gamma_2(\|v\|)\}$ .

The following theorem presents the nonlinear small-gain condition, which guarantees the ISS property of interconnected system (49) and (50).

**Theorem 5. ([34])** Under Assumption 2, if the following small-gain condition holds:

$$\chi_1 \circ \chi_2(s) < s \quad \forall s > 0, \quad (54)$$

then the interconnected system (49) and (50) is ISS with respect to  $v$  as the input.

## REFERENCES

- [1] A. Eidehall, J. Pohl, F. Gustafsson, and J. Ekmark, "Toward autonomous collision avoidance by steering," *IEEE Transactions on Intelligent Transportation Systems*, vol. 8, pp. 84–94, March 2007.
- [2] V. Cerone, M. Milanese, and D. Regruto, "Combined automatic lane-keeping and driver's steering through a 2-dof control strategy," *IEEE Transactions on Control Systems Technology*, vol. 17, pp. 135–142, Jan 2009.
- [3] R. Rajamani, H.-S. Tan, B. K. Law, and W.-B. Zhang, "Demonstration of integrated longitudinal and lateral control for the operation of automated vehicles in platoons," *IEEE Transactions on Control Systems Technology*, vol. 8, pp. 695–708, Jul 2000.
- [4] E. Wiener and R. Curry, "Flight-deck automation: promises and problems," *Ergonomics*, vol. 23, no. 10, pp. 995–1011, 1980.
- [5] M. Flad, L. Frhlich, and S. Hohmann, "Cooperative shared control driver assistance systems based on motion primitives and differential games," *IEEE Transactions on Human-Machine Systems*, vol. 47, pp. 711–722, Oct 2017.
- [6] H. E. B. Russell, L. K. Harbott, I. Nisky, S. Pan, A. M. Okamura, and J. C. Gerdes, "Motor learning affects car-to-driver handover in automated vehicles," *Science Robotics*, vol. 1, no. 1, 2016.
- [7] L. Saleh, P. Chevrel, F. Claveau, J. F. Lafay, and F. Mars, "Shared steering control between a driver and an automation: Stability in the presence of driver behavior uncertainty," *IEEE Transactions on Intelligent Transportation Systems*, vol. 14, pp. 974–983, June 2013.
- [8] S. J. Anderson, S. C. Peters, T. E. Pilutti, and K. Iagnemma, "An optimal-control-based framework for trajectory planning, threat assessment, and semi-autonomous control of passenger vehicles in hazard avoidance scenarios," *International Journal of Vehicle Autonomous Systems*, vol. 8, no. 2-4, pp. 190–216, 2010.
- [9] S. Zafeiropoulos and P. Tsiotras, "Design of a lane-tracking driver steering assist system and its interaction with a two-point visual driver model," in *American Control Conference*, pp. 3911–3917, June 2014.
- [10] S. M. Erlien, S. Fujita, and J. C. Gerdes, "Shared steering control using safe envelopes for obstacle avoidance and vehicle stability," *IEEE Transactions on Intelligent Transportation Systems*, vol. 17, pp. 441–451, Feb 2016.
- [11] W. Wang, J. Xi, C. Liu, and X. Li, "Human-centered feed-forward control of a vehicle steering system based on a driver's path-following characteristics," *IEEE Transactions on Intelligent Transportation Systems*, vol. 18, pp. 1440–1453, June 2017.
- [12] A. Nguyen, C. Sentouh, and J. Popieul, "Sensor reduction for driver-automation shared steering control via an adaptive authority allocation strategy," *IEEE/ASME Transactions on Mechatronics*, vol. 23, pp. 5–16, Feb 2018.
- [13] J. Jiang and A. Astolfi, "Shared-control for a rear-wheel drive car: Dynamic environments and disturbance rejection," *IEEE Transactions on Human-Machine Systems*, vol. 47, pp. 723–734, Oct 2017.
- [14] Z. Ercan, A. Carvalho, M. Gokasan, and F. Borrelli, "Modeling, identification, and predictive control of a driver steering assistance system," *IEEE Transactions on Human-Machine Systems*, vol. 47, pp. 700–710, Oct 2017.
- [15] S. H. Tamaddoni, S. Taheri, and M. Ahmadian, "Optimal preview game theory approach to vehicle stability controller design," *Vehicle System Dynamics*, vol. 49, no. 12, pp. 1967–1979, 2011.
- [16] X. Na and D. J. Cole, "Game-theoretic modeling of the steering interaction between a human driver and a vehicle collision avoidance controller," *IEEE Transactions on Human-Machine Systems*, vol. 45, pp. 25–38, Feb 2015.
- [17] D. D. Salvucci and R. Gray, "A two-point visual control model of steering," *Perception*, vol. 33, no. 10, pp. 1233–1248, 2004.
- [18] S. Schnelle, J. Wang, H. J. Su, and R. Jagacinski, "A personalizable driver steering model capable of predicting driver behaviors in vehicle collision avoidance maneuvers," *IEEE Transactions on Human-Machine Systems*, vol. 47, pp. 625–635, Oct 2017.
- [19] D. P. Bertsekas, *Dynamic programming and optimal control*. Belmont, MA: Athena Scientific, 1995.
- [20] R. S. Sutton and A. G. Barto, *Reinforcement learning: an introduction*. Cambridge: MIT press, 1998.
- [21] F. L. Lewis and D. Vrabie, "Reinforcement learning and adaptive dynamic programming for feedback control," *IEEE Circuits and Systems Magazine*, vol. 9, no. 3, pp. 32–50, 2009.
- [22] Z. P. Jiang and Y. Jiang, "Robust adaptive dynamic programming for linear and nonlinear systems: An overview," *European Journal of Control*, vol. 19, no. 5, pp. 417 – 425, 2013.
- [23] T. Bian and Z. P. Jiang, "Value iteration and adaptive dynamic programming for data-driven adaptive optimal control design," *Automatica*, vol. 71, pp. 348 – 360, 2016.
- [24] W. Gao and Z. P. Jiang, "Adaptive dynamic programming and adaptive optimal output regulation of linear systems," *IEEE Transactions on Automatic Control*, vol. 61, pp. 4164–4169, Dec 2016.
- [25] Y. Jiang and Z. P. Jiang, *Robust Adaptive Dynamic Programming*. Hoboken NJ: Wiley-IEEE Press, 2017.
- [26] W. Gao and Z. P. Jiang, "Learning-based adaptive optimal tracking control of strict-feedback nonlinear systems," *IEEE Transactions on Neural Networks and Learning Systems*, vol. 29, pp. 2614–2624, June 2018.
- [27] W. Gao, Z. P. Jiang, and K. Ozbay, "Data-driven adaptive optimal control of connected vehicles," *IEEE Transactions on Intelligent Transportation Systems*, vol. 18, pp. 1122–1133, May 2017.
- [28] M. Huang, W. Gao, and Z. P. Jiang, "Connected cruise control with delayed feedback and disturbance: An adaptive dynamic programming approach," *International Journal of Adaptive Control and Signal Processing*, 2017. doi: 10.1002/acs.2834.
- [29] Z. Bien and J.-X. Xu, eds., *Iterative Learning Control: Analysis, Design, Integration and Applications*. Norwell, MA, USA: Kluwer Academic Publishers, 1998.
- [30] D. A. Bristow, M. Tharayil, and A. G. Alleyne, "A survey of iterative learning control," *IEEE Control Systems*, vol. 26, pp. 96–114, June 2006.
- [31] N. Amann, D. H. Owens, and E. Rogers, "Iterative learning control using optimal feedback and feedforward actions," *International Journal of Control*, vol. 65, no. 2, pp. 277–293, 1996.
- [32] D. Owens and J. Htnen, "Iterative learning control an optimization paradigm," *Annual Reviews in Control*, vol. 29, no. 1, pp. 57 – 70, 2005.
- [33] Z. P. Jiang, A. R. Teel, and L. Praly, "Small-gain theorem for ISS systems and applications," *Mathematics of Control, Signals and Systems*, vol. 7, no. 2, pp. 95–120, 1994.
- [34] Z. P. Jiang, I. M. Mareels, and Y. Wang, "A Lyapunov formulation of the nonlinear small-gain theorem for interconnected ISS systems," *Automatica*, vol. 32, no. 8, pp. 1211 – 1215, 1996.
- [35] R. Rajamani, *Vehicle Dynamics and Control*. Springer Science and Business Media, 2011.
- [36] C. Sentouh, B. Soualmi, J. C. Popieul, and S. Debernard, "Cooperative steering assist control system," in *IEEE International Conference on Systems, Man, and Cybernetics*, pp. 941–946, Oct 2013.
- [37] G. Markkula, O. Benderius, and M. Wahde, "Comparing and validating models of driver steering behaviour in collision avoidance and vehicle stabilisation," *Vehicle System Dynamics*, vol. 52, no. 12, pp. 1658–1680, 2014.
- [38] C. Sentouh, P. Chevrel, F. Mars, and F. Claveau, "A sensorimotor driver model for steering control," in *IEEE International Conference on Systems, Man and Cybernetics*, pp. 2462–2467, Oct 2009.
- [39] J. Huang, *Nonlinear Output Regulation: Theory and Applications*. Philadelphia, PA: SIAM, 2004.
- [40] F. L. Lewis, D. L. Vrabie, and V. L. Syrmos, *Optimal control*. John Wiley & Sons, 3rd ed., 2012.
- [41] H. K. Khalil, *Nonlinear Systems*. Prentice-Hall, 2002.
- [42] G. Zames, "On the input-output stability of time-varying nonlinear feedback systems part one: Conditions derived using concepts of loop gain, conicity, and positivity," *IEEE Transactions on Automatic Control*, vol. 11, pp. 228–238, Apr 1966.
- [43] D. Kleinman, "On an iterative technique for Riccati equation computations," *IEEE Transactions on Automatic Control*, vol. 13, pp. 114–115, Feb 1968.
- [44] MATLAB, version 9.0.0 (R2016a). Natick, Massachusetts: The Math-Works Inc., 2016.
- [45] E. D. Sontag, "Smooth stabilization implies coprime factorization," *IEEE Transactions on Automatic Control*, vol. 34, pp. 435–443, Apr 1989.
- [46] E. D. Sontag and Y. Wang, "On characterizations of the input-to-state stability property," *Systems & Control Letters*, vol. 24, no. 5, pp. 351 – 359, 1995.